*Brazilian Journal of Physics, vol. 24, no. 1. March. 1994*

# Raman Study of Strain Effects on [100] and [111] Oriented $GaAs/CaF_2$ Heterostructures

P. S. Pizani
*Departamento de Física, Universidade Federal de São Carlos*
*Caixa Postal 676, 13565-905 São Carlos, SP, Brasil*

C. Fontaine
*Laboratoire d'Automatique et d'Analyse des Systèmes*
*7 Av. Colonel Roche, 31077 Toulouse Cedex, France*

R. Carles
*Laboratoire de Physique des Solides, Université Paul Sebatier*
*118 Route de Narbonne, 31062 Toulouse Cedes, France*

Received July 12, 1993; revised manuscript received October 29, 1993

Raman spectroscopy is used to study the strain profile in thin layers of GaAs grown on $CaF_2$ substrate by molecular beam epitaxy. The strain is deduced from the frequency shift of the long wavelength transverse and longitudinal optical phonons. Due to transparency of the substrate, it was possible to perform measurements on both sides of the semiconducting layer. The strain relaxation profile was mesured changing the exciting wavelength, i.e., the penetration depth of the light. A comparative discussion is made for samples of GaAs thin layer growth in the [100] and [111] directions.

## I. Introduction

Strain effects on semiconducting materials has been studied several years ago, by the use of various optical technics as photoluminescence, electrorefletance or Raman spectroscopy[1–3], etc.

More recently, with the appearance of the crystalline thin films epitaxially grown by molecular beam epitaxy (MBE), or metalorganic chemical vapour deposition (MOCVD), studies of the strain effects in a large variety of semiconductor heterostructures have been performed[4–6]. In these cases, the stress originates in the difference between the lattice parameters and/or between the thermal expansion coefficients of the substrate and epitaxial layer. Several methods have been developped to minimize the resulting lattice mismatch in order to improve the crystalline quality of the semiconductor film, since the strain relaxation produces crystalline defects which impair its transport and optical properties, thus the possible device applications. Nevertheless, there are also very interesting applications in the case of the highly strained semiconductor thin films. As an example, in a strained semiconductor like GaAs, the $k \sim 0$ splitting of the upper valence bands opened the possibility of efficiency improvement by the use of the highly strained GaAs thin films (with a surface treated to obtain a negative electron affinity) as a polarized electron source[7–9].

Very high strain effects can be obtained in heterostructures as GaAs grown on $CaF_2$, due to the large difference between their thermal expansion coefficients. In this work, Raman spectroscopy is used to study these strain effects. The influence of the growth direction ([100] or [111]) on residual stresses was mesured. Since the substrate is transparent, measurements can be performed on both sides of the semiconducting layer, namely at the free surface and the interface. Furthermore, changing the energy of the incident light (i.e. the penetration depth) it was possible to analyze the stress

Table I. Theoretical values of the frequency shift $\Delta\omega$ ($\mathrm{cm}^{-1}$) as a function of the stress $X(GP_a)$ for the GaAs.

| Mode | $\Delta\omega(\mathrm{cm}^{-1})[100]$ | $\Delta\omega(\mathrm{cm}^{-1})[111]$ |
|---|---|---|
| LO$_S$ | 3.9 X | 1.9 X |
| TO$_D$ | 2.7 X | 4.0 X |
| LO$_D$ | 2.3 X | 2.4 X |
| TO$_S$ | 3.3 X | 2.6 X |

relaxation profile along the growth direction.

## II. Strain effects on phonon frequency

The frequency changes of the long wavelength transverse (TO) and longitudinal optical (LO) phonon induced by a biaxial stress can be calculated by conventional procedures given in several references[10,11]. Particularly, when high symmetry directions are involved, one gets:

$$\Delta\omega_s = \frac{\omega_0}{2}[2(\tilde{k}_{11} + \tilde{k}_{12})S_{12} + 2\tilde{k}_{12}S_{11}] \cdot X \qquad (1)$$

$$\Delta\omega_D = \frac{\omega_0}{2}[2(\tilde{k}_{11} + \tilde{k}_{12})S_{12} + (\tilde{k}_{11} + \tilde{k}_{12})S_{11}] \cdot X \qquad (2)$$

for [100] direction[12], and

$$\Delta\omega_S = \frac{\omega_0}{3}[(\tilde{k}_{11} + 3\tilde{k}_{12})(S_{11} + 2S_{12}) - \tilde{k}_{44}S_{44}] \cdot X \qquad (3)$$

$$\Delta\omega_D = \frac{\omega_0}{3}[(k_{11} + 3k_{12})(S_{11} + 2S_{12}) + \frac{1}{2}\tilde{k}_{44}S_{44}] \cdot X \qquad (4)$$

for [111] direction. In these equations, $\Delta\omega$ is the frequency shift of the phonons, the subscripts $S$ an $D$ refer to the singlet or doublet modes, X is the stress, $\omega_0$ is the frequency of the $k \sim 0$ optical phonons in the absence of stress, the $\tilde{k}_{ij}$'s are the phonon deformation potentials and the $S_{ij}$'s are the elastic compliance constants referred to the cubic axes.

For the GaAs case, by using parameters available in the literature[13], we derived from equations (1)-(4) the frequency shifts $\Delta\omega$ (in $\mathrm{cm}^{-1}$) as a functions of the stress $X$ (in $GP_a$). Their values are reported in Table 1.

## III. Experimental

### III.1 - Samples preparation

GaAs has a face centered cubic crystalline structure with a lattice parameter value of 5.65Å $CaF_2$ and $SrF_2$ also present a cubic structure but their lattice parameters are equal to 5.46Å and 5.80Å respectively. So, a mixed $(Ca_{1-x}, Sr_x)F_2$ buffer layer with a convenient value of $x$ was MBE-grown between the $CaF_2$ substrate and the GaAs layer in order to allow the lattice matching. This provides a way of reducing the strain effects in comparison with GaAs thin films directly grown on $CaF_2$. However, the linear expansion coefficients of the fluorides and GaAs are very different, about $18 \times 10^{-6}$/K and 6 x $10^{-6}$/K respectively. Then, we expect more and more compressive stress when the temperature of the sample is lowered after growth to the room temperature value.

In this work, we have used 2.0 $\mu$m - thick GaAs layer on a 150 nm-tick $(Ca_{1-x}, Sr_x)F_2$ buffer layer grown by MBE at 550°C[14,15]. The same growth procedure was used for both [100] and [111] orientations of the $CaF_2$ substrate.

### III.2 - Raman measurements

The Raman measurements were performed with a T800 Coderg triple monochromator coupled with a cooled GaAs photomultiplier and a conventional photon counting system. All measurements were performed at room temperature. In order to avoid overheating of the samples, the output power of the laser was kept within 100 mw and the incident beam was focussed with a cylindrical lens. To observe the normally forbidden TO mode on a [100] oriented sample[16] a grazing incidente was used to break down the true backscattering geometry inside the sample. Indeed using the Raman selection rules, the relative intensities of the LO$_S$ and TO$_D$ modes, 1 and 0 for normal incidence, are replaced by $\cos^2(38/2)$ and $\sin^2\theta + \sin^2 38/2$, respectively, for an incidence angle $\theta$ inside the sample. The relative activation of the TO$_D$ is about 10% in GaAs[12].

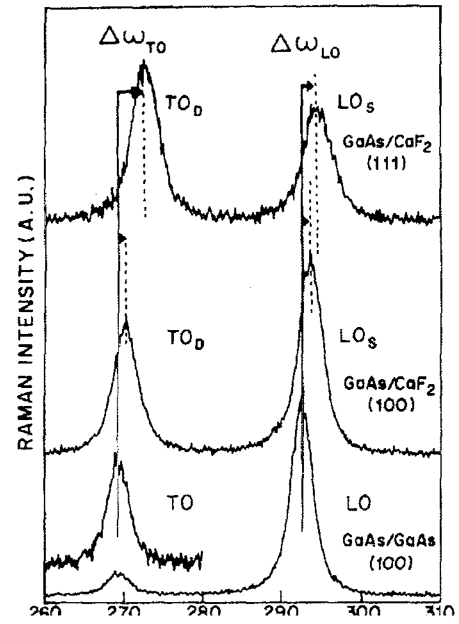

Figure 1: Raman spectra of the surface of the GaAs/CaF$_2$ epilayer growth in both directions [100] and [111] and GaAs/GaAs homoepitaxy as reference. The 406.8in exciting wavelength was used.

The Raman spectra were recorded using the 488.0nm argon ion and 647.1nm and 406.8nm kripton ion laser lines. The purpose was to explore different depths inside the GaAs films, since the penetration depth of the light is given by $\sim [2\alpha(\lambda)]^1$, where $\alpha(\lambda)$ is the absorption coefficient of the incident light[17]. For GaAs, the penetration depth is about 811111, 40nm and 140nm for the 406.8nm, 488.0nm and 647.1nm wavelengths, respectively.

The frequency shifts were always deduced from the comparison with the spectrum of a. homoepitaxial sample of GaAS simultaneously mounted on the sample holder.

## IV. Results and discussions

Figure 1 shows the Raman spectra recorded from the [100]- and [111]- oriented GaAs/CaF$_2$ samples, and the homoepitaxial reference sample. In order to observe the strain effects at the vicinity of the surface of the film, the 406.8nm laser line was used, since the penetration depth is reduced to about 8nm in this case.

The values of the stresses are given by

$$\Delta\omega_{TO}(cm^{-1}) = 2.7X(GP_a)$$

$$\Delta\omega_{LO}(cm^{-1}) = 3.9X(GP_a)$$

for the [100] directions, and

$$\Delta\omega_{TO}(cm^{-1}) = 4.0X(GP_a)$$

$$\Delta\omega_{LO}(cm^{-1}) = 1.9X(GP_a)$$

for the [111] direction.

From the values of the frequencies shifts measured on the spectra of Fig.1, we obtains X $\sim 1GP_a$ for the [111] direction and X $\sim 0.5GP_a$ for the [100] direction.

Figure 2 shows a typical spectra recorded from the surface and interface, for the GaAs/CaF$_2$ [111] direction, by using the 406.8nm, 488.0nm and 647.1nm laser lines. The penetration depth for each wavelength is plotted on the figure. At the bottom of this figure, the insert schematizes the experimental configuration used to record the signal a.t the vicinity of the interface. In this case, the Raman signal of the GaAs layer appears in the low frequency tail of the intense CaF$_2$ peak centered at 322 cm$^{-1}$. That explains the appearent background increase versus frequency on the corresponding spectra.

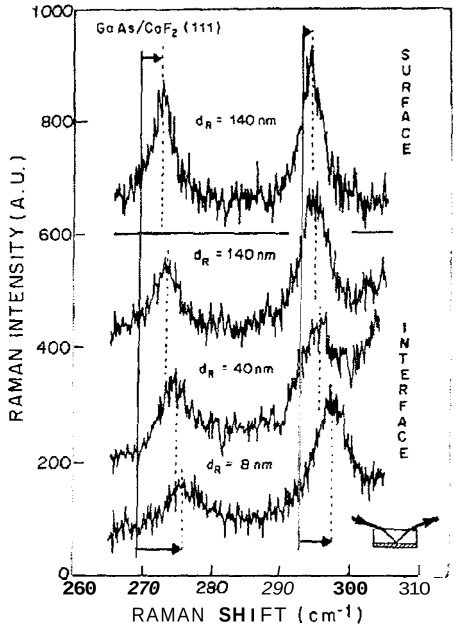

Figure 2: Raman spectra of the surface and interface of the GaAs/CaF$_2$ heterostructure for three exciting wavelengths. $d_R$ is the Raman depth.

Figure 3 shows the values of the stress as a function of the light penetration depth, mesured for both samples [100] and [111] directions and for both sides of *the semiconducting films* (surface and *interface*). This figure shows that the stress values deduced from either the TO or LO mode rather well coincide, far from the interface, if the uncertainties on the $K'_{ij}$ parameters are taken into account. On the contrary, one notes that the nearer the interface is, the larger the discrepancies are. This is due to the large amount of defects in that zone (see the large broadening of the Raman peaks in Fig. 2). In fact, it is interesting to remark that the Raman spectrum was hidden by an intense quasi-elastic scattering at the [100] interface for the case of the 406.8nm exciting-laser line. This shows evidence of the poor crystalline quality of the [100] interface in comparison with the [111] interface. Hence, the lost of translational symmetry allows the activation of the LO$_D$ (or TO$_S$), leading thus to overestimate (or underestimate) the stress value from the LO (or TO) shift for the [111] direction and the inverse phenomenon for the [100] direction (see Table I). in good accordance with the observations.

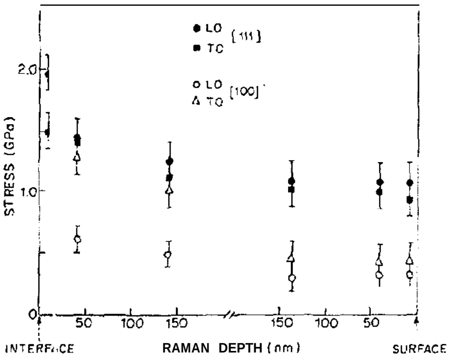

Figure 3: The values of the stress at the interface and surface of the GaAs epilayer growth on CaF$_2$ for [100] and [111] directions as a function of the Raman depth ($d_R$).

Finally, from our experimental data, we can draw some interesting results: (i) the relatively high value of the residual stress at the surface means that this type of heterostructure is very promising for valence band engineering devices, like polarized eletrons sources; (ii) the residual stress is more important for the [111] growth direction than for the [100] one; (iii) we have observed that the stress have a very high value at the interface compared with those at the surface, for both growth directions; (iv) the stress relaxation process is very important in regions near to the interface: it takes place in the *first* $\sim 200\AA$ *from* the interface.

## Acknowledgments

The authors would like to thank the Brazilian Agencies FAPESP and CNPq-RHAE for financial support.

## References

1. H. Mathieu, P. Merle, E. L. Ameziane, B. Archilla and J. Camassel, Phys. Rev. B19, 2209 (1979).
2. F. H. Pollak and M. Cardona, Phys. Rev., **172,** 816 (1968).
3. E. Anastassakis, A. Pinczuk, E. Burnstein, F. H. Pollak and M. Cardona, Solid State Commun. **8,** 133 (1970).
4. G. Landa, R. Carles, C. Fontaine, E. Bedel and A. Munõz-Yagüe, J. Appl. Phys. 66, 196 (1989).
5. G. Abstreiter, E. Bauser, A. Fiscker and K. Ploog, Appl. Phys. 16, 345 (1978).
6. G. Landa, R. Carles, J. B. Renucci, C. Fontaine, E. Bedel and A. Munõz-Yagüe, J. Appl. Phys. 60, 1025 (1986).
7. G. Lampel and C. Weisbuch, Solid State Commun. 16, 877 (1975).
8. V. M. Agranovich and A. A. Maradudin *Optical Orientation*, (North Holland, Amsterdam, 1984) Vol.8.
9. E. Daran, C. Fontaine, A. Muñoz-Yague, I. Lassailly, C. Hermann, R. Carles et P. S. Pizani, Journées Electronique III-V (La Grande Motte, France 1992).
10. E. Anastassakis, A. Pinczuk, E. Burnstein, F. H. Pollak and M. Cardona, Solid State Commun. **8,** 133 (1970).
11. F. Cerdeira, C. J. Buchenauer, F. H. Pollak and M. Cardona, Phys. Rev. B5, 580 (1972).
12. G. Landa, R. Carles, C. Fontaine, E. Bedel and A. Munõz-Yagüe, J. Appl. Phys. 66, 196 (1989).
13. P. Wickboldt, E. Anastassakis, R. Sauer and M. Cardona, Phys. Rev. B35, 1362 (1987).
14. S. Siskos, C. Fontaine and A. Munoz-Yague, Appl. Phys. Lett 44, 1146 (1984).
15. C. Fontaine, H. Benarfa, E. Bedel, A. Munõz-Yagüe, G. Landa and R. Carles, J. Appl. Phys. 60, 208 (1986).
16. M. Cardona in *Light Scattering in Solids II* (Springer, Berlin 1982) p. 49.
17. D. E. Aspnes and A. A. Studna, Phys. Rev. B 22, 985 (1983).